Total Inhibition of the Oxygen Reduction Reaction at Au(111) by Copper Adlayers in Sulfuric Acid Solution

Takayuki ABE, Youichiro MIKI, and Kingo ITAYA*
Department of Engineering Science, Faculty of Engineering, Tohoku University, Sendai 980
(Received February 28, 1994)

The influence of an underpotentially deposited adlayer of copper on the oxygen reduction reaction (ORR) at Au(111) has been studied in a 0.05 M H_2SO_4 solution using hanging meniscus rotating disk voltammetry. The total inhibition of the ORR was found after the formation of the first Cu adlayer. Two possible structures for the Cu adlayer on Au(111) take into account inhibition of the ORR. The total inhibition observed in the present study can be explained by a honeycomb ($\sqrt{3}\times\sqrt{3}$)R30° structure, rather than a simple ($\sqrt{3}\times\sqrt{3}$)R30° Cu adlayer. A bridging two-site process (disproportionation reaction) is not expected to occur on the honeycomb Cu adlayer.

The oxygen reduction reaction (ORR) kinetics shows a pronounced effect on the atomic structure of the electrode surface. The effect of the electrode's crystallographic orientation on the ORR has recently been investigated at well-defined Au and Pt single-crystal electrodes.[1—3] It is also well-known that foreign metal adlayers strongly influence the ORR kinetics, as well as several other electrochemical reactions.[1,2]

Correlations between the surface structure of adlayer-modified electrodes and the observed electrocatalytic activity are of special importance for understanding the structure-reactivity relationship at the atomic level. In situ scanning tunneling microscopy (STM), atomic force microscopy (AFM) and X-ray analysis are now recognized as being important techniques for the in situ atomic-level characterization of electrode surfaces.[4] Chen et al. have recently discussed the correlation between underpotentially deposited (UPD) Bi on Au(111) and the H_2O_2 reduction.[5] In our recent paper, the effect of the Cu UPD on the ORR was discussed concerning Pt(111) in an aqueous sulfuric acid solution.[6]

In this paper we report on the near total inhibition of the ORR at Au(111) surfaces modified with Cu adlayers in a sulfuric acid solution using hanging meniscus rotating disk (HMRD) voltammetry. It has recently been reported that the images obtained by in situ STM and AFM for the first Cu adlayer on Au(111) in a sulfuric acid solution exhibit the ($\sqrt{3}\times\sqrt{3}$)R30° ordered structure.[7—9] The reduction current for oxygen is greatly suppressed by the formation of the first Cu UPD. We now propose a possible mechanism for the inhibition of the ORR at Au(111) in the presence of a Cu adlayer.

Experimental

Single crystals of Au were prepared at the end of a Au wire by Clavilier's method.[10,11] The crystallographic axes were determined by means of a laser-beam reflection technique. As a final treatment, well-defined surfaces were exposed by a flame-anneal quenching technique, as described in previous literature.[8,10,11]

HMRD voltammetry using a semi-spherical single-crystal electrode was employed for studying the ORR. A detail description of this experiment was reported in our recent paper.[6] A linear behavior in Levich plots for the reduction of hexacyanoferrate(III) was observed at an Au(111) electrode up to a rotation rate of 3000 rpm. However, a slow rotation rate of 200 rpm was employed in the present HMRD experiment for the ORR in order to avoid any accumulation of small amounts of contaminants on the clean surface.[12]

All potentials are reported with respect to a reversible hydrogen electrode (RHE) in a 0.05 M H_2SO_4 solution (1 M=1 mol dm^{-3}). All of the solutions used were prepared using ultrapure water (Millipore-Q).

Results and Discussion

Figure 1 shows a cyclic voltammogram of a Au(111) surface obtained in a 0.05 M H_2SO_4 solution. Two separate peaks for the oxidation of Au(111) are observed on the anodic scan at 1.4 V and 1.57 V vs. RHE. A reduction peak at ca. 1.12 V is observed on the cathodic scan due to the reduction of oxide layers formed on the Au(111) surface. A hydrogen evolution reaction commences at potentials more negative than −0.15 V vs. RHE. A similarly shaped voltammogram was reported in a previous paper from our laboratory.[8]

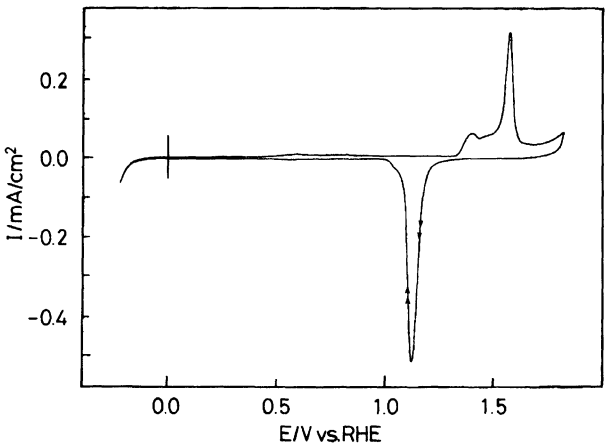

Fig. 1. A cyclic voltammogram for a Au(111) electrode in a nitrogen saturated 0.05 M H_2SO_4 solution. The scan rate was 50 mV s^{-1}.

Figure 2-A shows steady-state current-potential curves at Au(111) obtained by the HMRD experiment in an oxygen-saturated 0.05 M H_2SO_4 solution at a rotation speed of 200 rpm. The current-potential curves of a, b, and c in Fig. 2-A were measured by changing the sensitivity in the current scale, respectively. The individual points were obtained by sampling the current at each potential after a holding period of 15 s so as to eliminate any effect of the background charging current. The ORR current commences at ca. 0.7 V vs. RHE, and gradually increases in the potential region between 0.7 V and −0.1 V. A steady-state current-potential curve obtained by the HMRD experiment in a nitrogen-saturated 0.05 M H_2SO_4 solution at the same rotation speed is also shown in Fig. 2-A (solid circles). No significant current was observed through the entire potential region between 0.7 V and −0.1 V in a nitrogen-saturated solution. An increase in the reduction current due to hydrogen evolution was observed to commence at potentials more negative than −0.1 V. It has been observed that the ORR current begins to flow at 0.9 V vs. RHE on a well-defined Pt(111), and reaches a limiting current of ca. 2 mA cm^{-2} at 0.5 V vs. RHE under an identical experimental condition with the same rotation speed.[6] The observed limiting current of ca. 2 mA cm^{-2} on the Pt(111) has been explained by a direct $4e^-$ reduction to form water according to the following reaction, when it is assumed that the oxygen concentration in the solution is 1.2 mM[13] and the diffusion coeffiecent of oxygen is 2.0×10^{-5} $cm^2\,s^{-1}$;[14]

$$O_2 + 4H^+ + 4e^- \rightarrow 2H_2O \quad (1)$$

Although no mass-transport limited ORR current was clearly observed on Au(111), as shown in Fig. 2-A (curve a), the ORR current observed at potentials more negative than 0 V became nearly equal to the limiting value of ca. 2 mA cm^{-2} for the $4e^-$ reaction. This observation strongly suggests that the ORR on a well-defined Au(111) also proceeds by an overall $4e^-$ transfer at potentials more negative than 0 V vs. RHE.

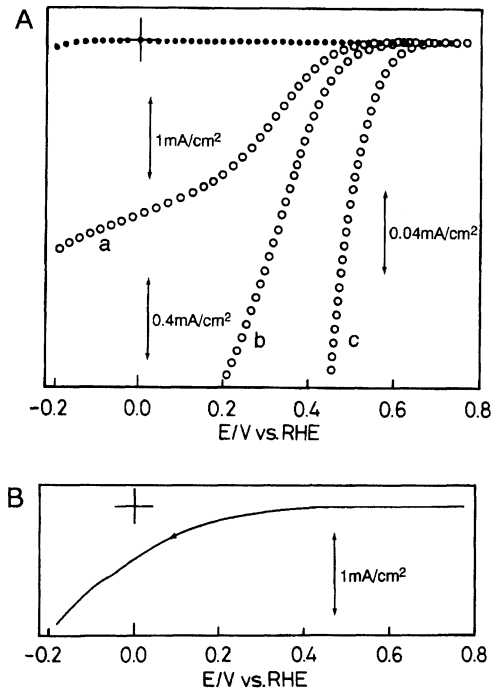

Fig. 2. (A) Steady-state current–potential curves (a, b, and c) for the oxygen reduction reaction at Au(111) observed with different sensitivities as indicated in an oxygen saturated 0.05 M H_2SO_4 solution. Rotation speed was 200 rpm. Solid circules indicate a background current–potential curve in a nitrogen saturated 0.05 M H_2SO_4 solution. (B) A current-potential curve for H_2O_2 reduction at Au(111) in an nitrogen saturated 0.05 M H_2SO_4 solution in the presence of 5 mM H_2O_2. The scan rate was 1 mV s^{-1}.

Figure 2-B shows a current-potential curve at Au(111) in a nitrogen-saturated 0.05 M H_2SO_4 solution containing 5 mM H_2O_2 at a scan rate of 1 mV s^{-1}. It can been seen in Fig. 2-B that the reduction current of H_2O_2 commences at ca. 0.3 V, and slowly increases at more negative potentials. Adzic and co-workers reported that hydrogen peroxide (H_2O_2) is the final reduction product at Au(111) in an alkaline solution.[1] We therefore suppose that the ORR at Au(111) proceeds by a $2e^-$ transfer to form H_2O_2 at potentials more positive of 0.3 V vs. RHE. At more negative potentials than 0.3 V, the intermediate product (H_2O_2) can be further reduced to water, leading to an overall $4e^-$ transfer reaction. The reaction mechanism has been described as follows:[15]

⟨one site process⟩

$$M + O{=}O \xrightarrow{e^-+H^+} M{-}O{-}OH \xrightarrow{e^-+H^+} M + H_2O_2 \quad (2)$$

⟨bridging two sites process⟩

$$M + 2O{=}O \xrightarrow{2e^-+2H^+} \begin{matrix} M \\ | \\ M{-}O{-}O{-}H \\ | \\ M{-}O{-}O{-}H \end{matrix} \longrightarrow M + O{=}O + H_2O_2 \quad (3)$$

Reaction (2) is expected to proceed at a single atomic adsorption site. On the other hand, two nearest-neighbor adsorption sites are necessary for the disproportionation reaction between two adsorbed species ($-O_2H$), as shown in reaction (3). Previous literature suggests that the two-site process is favorable on Au electrodes for the ORR.[15]

Figure 3-A shows a cyclic voltammogram for the underpotential deposition of Cu on Au(111) in 0.05 M H_2SO_4 containing 5 mM $CuSO_4$ at a scan rate of 1 mV s^{-1}. Two well-resolved deposition peaks can be clearly observed at 0.57 V and 0.38 V vs. RHE before bulk deposition commences at 0.34 V. The first Cu UPD peak at 0.57 V is narrow with a half-width of 5

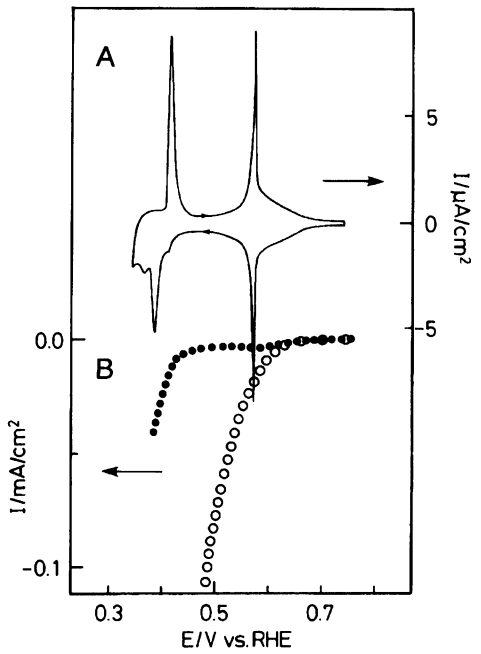

Fig. 3. (A) A cyclic voltamogram for a Au(111) electrode in a 0.05 M H_2SO_4 solution in the presence of 5 mM $CuSO_4$. The scan rate of the electrode potential was 1 mV s^{-1}. (B) A steady-state voltammogram for the oxygen reduction at Au(111) in an oxygen saturated 0.05 M H_2SO_4 in the presence of (solid circles) and absence of (open circles) 5 mM $CuSO_4$. Rotation speed was 200 rpm.

mV. The half-width of the second peak at 0.38 V is 15 mV. The voltammogram shown in Fig. 3-A is similar to that reported previously.[8]

Figure 3-B shows steady- state current- potential curves obtained by the HMRD voltammetry for the ORR at Au(111) in an oxygen-saturated 0.05 M H_2SO_4 solution in the presence of (solid circles) and the absence (open circles) of 5 mM $CuSO_4$. The first Cu UPD peak (ca. 0.57 V) is located near to the onset potential of the ORR at bare Au(111), as shown in Fig. 2-A. A near total inhibition in the ORR current can be observed after the first Cu UPD. The currents observed at 0.5 V vs. RHE were in the range of 4—8 μA cm^{-2} in the presence of a Cu adlayer, compared with 100 μA cm^{-2} at bare Au(111) electrodes at the same potential. Therefore, the small limiting current observed in between the first and second Cu UPD peaks is believed to be due to surface defects in the Cu adlayers or edge effects at the HMRD electrode. A further increase in the reduction current at potentials more negative than 0.4 V (solid circles in Fig. 3-B) is thought to be due to the bulk deposition of Cu^{2+} in an oxygen-saturated solution. It is obvious that a total inhibition of the ORR occurs after the formation of the first Cu adlayer on Au(111). The ORR current after the second Cu UPD was difficult to observed due to the bulk deposition of Cu, as mention above. However, it is reasonably expected that the ORR should also be inhibited after the second UPD.

Note that the near total inhibition of the ORR current after the formation of the first Cu adlayer on Au(111) is in contrast with the current response observed after the formation of the first Cu adlayer at Pt(111) in an oxygen-saturated 0.05 M H_2SO_4.[6] In the case of Pt(111), a steady-state ORR current was observed in the potential region between the first and second UPD peaks.[6] This steady-state current was nearly one half of the limiting current observed on bare Pt(111) at the same potential. This significant difference in the inhibition observed at Cu-modified Au(111) and Pt(111) can be explained by a difference in reaction pathways for the ORR.[6] The ORR on Pt with a Cu adlayer can be proceeded by a one-site process (Eq. 2) to form H_2O_2. On the other hand, the two-site process of Eq. 3 is expected on Au surfaces, as discussed above.

We previously reported a detailed study of the Cu UPD process on Au(111) in 0.05 M H_2SO_4 using in situ STM. The STM images showed a structure denoted by a simple $(\sqrt{3}\times\sqrt{3})R30°$, as described in previous papers.[7,8] An identical image has also been observed by in situ AFM.[9] Based on the STM and AFM observations, it has been assumed that the corrugation observed in images corresponds to individual copper adatoms (see Fig. 4-A). However, Shi and Lipkowski have recently proposed a new structure for Cu adlayers on Au(111) based on chronocoulometric measurements.[16,17] They proposed that the copper adatoms are packed in the shape of a honeycomb $(\sqrt{3}\times\sqrt{3})R30°$ structure with the centers of the honeycomb occupied by sulfate ions, as shown in Fig. 4-B. This model suggests that the ordered structure observed in the STM[7,8] and AFM[9] experiments corresponds to

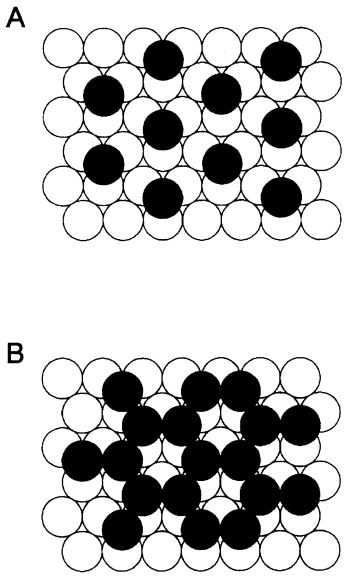

Fig. 4. Schematic representations of two possible surface structures of the Cu adlayer on a Au(111). Open and solid circles indicate Au and Cu atoms, respectively.

the images of co-adsorbed sulfate ions.

Although there appears to be some debate concerning the structure of the Cu adlayer on Au(111) (Fig. 4), the total inhibition of the ORR observed in this study can be explained, as follows:

(i) If anions such as sulfate or hydrogensulfate are more strongly adsorbed on Cu-modified Au(111) than oxygen molecules, the ORR can not be proceeded on the Cu-modified Au(111), because of the absence of reaction sites. The ORR is not expected to occur through Cu adatoms in the potential region examined here, because the ORR current found in this study began at potentials more negative of 0 V vs. RHE in an oxygen-saturated 0.05 M H_2SO_4 solution on a pure Cu metal electrode.

(ii) If the co-adsorbed anions can be partially replaced by oxygen, the adsorbed oxygen species ($-O_2H$) can be found at the position formerly occupied by the anion. In the honeycomb structure (Fig. 4-B), however, there would appear to be no nearest-neighbor adsorption site available to facilitate the disproportionation reaction (Eq. 3). The nearest distance between the adsorbed oxygen species ($-O_2H$) should be ca. 0.5 nm based on the honeycomb structure. In this case, the ORR can be totally inhibited by the Cu adlayer. On the other hand, there is a possibility to form two-nearest neighbor adsorbed oxygen species ($-O_2H$) within the simple $(\sqrt{3}\times\sqrt{3})R30°$ unit cell, although a simultaneous occupancy by two oxygen molecules at two hollow sites in the unit cell does not seem likely. However, the total inhibition of the ORR found in this study seems to be more appropriately explained by the honeycomb $(\sqrt{3}\times\sqrt{3})$-R30° structure proposed by Shi and Lipkowski.[16,17]

Conclusions

The present results demonstrate that the ORR can be employed as a simple catalytic reaction to provide a better understanding of how the chemical environment of the electrode surface affects the reactivity. The ORR on bare Au(111) in an oxygen-saturated 0.05 M H_2SO_4 solution was investigated by using HMRD voltammetry. The reduction current commenced at ca. 0.7 V vs. RHE, and then gradually increased in negative potentials. The ORR initially involved a $2e^-$ transfer reaction to form H_2O_2 in the potential region between 0.7 V and 0.3 V followed by a further reduction of H_2O_2 to H_2O at potentials more negative than 0.3 V. The ORR in the presence of the Cu adlayer on Au(111) was also examined by HMRD voltammetry. After the formation of the first Cu adlayer with the $(\sqrt{3}\times\sqrt{3})R30°$ structure, the reduction current was almost totally inhibited. The total inhibition of the ORR on Au(111) with a Cu adlayer can be explained by either (i) the blocking of oxygen adsorption sites on Au(111) or (ii) the inhibition of the disproportionation reaction due to the formation of a honeycomb structure.

This work was supported by Ministry of Education, Science and Culture, Grant-in-Aid for research (Nos. 04241103 and 05235205). The authors would like to express their thanks to Professor J. Lipkowski (Univ. Guelph, Canada) for sending us their papers prior to publication.[16,17]

References

1) R. R. Adzic, "Modern Aspects of Electrochemistry," ed by R. E. White, J. O'M. Bockris, and B. E. Conway, Plenum Press, New York and London (1990), Vol. 21, pp. 163—236.

2) G. Kokkinidis and D. Jannakoudakis, *J. Electroanal. Chem.*, **162**, 163 (1984).

3) F. El. Kadiri, R. Faure, and R. Durand, *J. Electroanal. Chem.*, **301**, 177 (1991).

4) A. J. Bard, H. D. Abruna, C. E. Chidsey, L. R. Faulkner, S. W. Feldberg, K. Itaya, M. Majda, O. Melroy, R. W. Murray, M. D. Porter, M. P. Soriaga, and H. S. White, *J. Phys. Chem.*, **97**, 7147 (1993).

5) C-h. Chen, K. D. Kepler, A. A. Gewirth, B. M. Ocko, and J. Wang, *J. Phys. Chem.*, **97**, 7290 (1993).

6) T. Abe, G. M. Swain, K. Sashikata, and K. Itaya, *J. Electroanal. Chem.*, submitted (1994).

7) O. M. Magnussen, J. Hotlos, G. Beitel, D. M. Kolb, and R. J. Behm, *J. Vac. Sci. Technol.*, **B9**(2), 969 (1991).

8) T. Hachiya, H. Honbo, and K. Itaya, *J. Electroanal. Chem.*, **315**, 275 (1991).

9) S. Manne, P. K. Hansma, J. Massie, V. B. Elings, and A. A. Gewirth, *Science*, **251**, 183 (1991).

10) J. Clavilier, A. Rodes, K. El. Achi, and M. A. Zamakhchari, *J. Chim. Phys.*, **88**, 1291 (1991).

11) S. Motoo and N. Furuya, *J. Electroanal. Chem.*, **172**, 339 (1984).

12) B. D. Cahan, H. M. Villullas, and E. B. Yeager, *J. Electroanal. Chem.*, **306**, 213 (1991).

13) N. M. Markovic, R. R. Adzic, and V. B. Vesovic, *J. Electroanal. Chem.*, **165**, 121 (1984).

14) D. R. Lawson, L. D. Whiteley, C. R. Martin, M. N. Szentirmay, and J. I. Song, *J. Electrochem. Soc.*, **135**, 2247 (1988).

15) J. C. Huang, R. K. Sen, and E. B. Yeager, *J. Electrochem. Soc.*, **126**, 786 (1979).

16) Z. Shi and J. Lipkowski, *J. Electroanal. Chem.*, **364**, 289 (1994).

17) Z. Shi and J. Lipkowski, *J. Electroanal. Chem.*, **365**, 303 (1994).